Kuwait J. Sci. **46 (3)** pp. 53-59, 2019

Dielectric properties of sintered $BaTiO_3$ prepared from barium acetate and titanium dioxide

Kolthoum I. Othman[1,*] M. El Sayed Ali[1] and S. El-Hout[1]

[1] *Metallurgy Dept., NRC, Atomic Energy Authority, Cairo, Egypt.*

* *Corresponding author: Kolthoum.O@yahoo.com*

Abstract

We investigated the densification, microstructure and dielectric properties of $BaTiO_3$ derived from aqueous barium acetate and titanium dioxide mixture in both the unmilled and milled forms. The sintered pellets showed a great difference in the microstructure and dielectric properties between the milled and unmilled ones. The unmilled samples displayed broadening in the permittivity peaks at Curie temperature and a higher permittivity value (5630) at room temperature. They exhibit a dielectric relaxor-like behavior and relatively stable permittivity. This was attributed to the presence of a thin shell layer of barium-rich phase at the grain boundaries. It was found that although milling gives a better homogeneity, it destroys the shell layer and results in classic barium titanate dielectric behavior.

Keywords: Barium titanate; barium acetate; dielectric properties; sintering & microstructure.

1. Introduction

Barium titanate ($BaTiO_3$) ferroelectric ceramic has been extensively studied during the last decades due to its excellent dielectric, ferroelectric and piezoelectric properties. These properties make it very useful in many applications, such as capacitors, multilayer ceramic capacitors (MLCCs), PTC thermistors, piezoelectric transducers, and a variety of electro-optic devices (Ertuğ, 2013). In addition, it has been used as a photocatalyst because of its composition containing TiO_2. The latter possesses' excellent photocatalytic activity (Zheng, 2016). Several synthesis methods (i.e., solid-state reaction, hydrothermal, sol gel, co-precipitation and others) have been used to prepare $BaTiO_3$ powder (Li *et al*., 2002; Rotaru *et al*., 2017; Vijatović *et al*., 2008). It has been reported that, the synthesis method has significant effects on the structure and properties of barium titanate material. The synthesis method is not the only one that has these effects. Sintered density, grain size and phases at the grain boundary also have a great effect on the structure and dielectric properties of sintered $BaTiO_3$ (Vijatović *et al*., 2008). As miniaturization of electronic devices requires powders with smaller particle size that have controlled morphology, various wet-chemical methods have been used to produce nano-size barium titanate (Luan *et al*., 2004; Peng, *et al*., 2003; Kim *et al*., 2004; Gomes *et al*., 2018). The mechanical activation of starting precursors is also a very effective method for obtaining fine $BaTiO_3$ powders (Kong *et al*., 2002).

In this study, a low cost and simple method was used to prepare $BaTiO_3$ fine powder through homogeneous coating of TiO_2 particles with barium acetate solution. The mechanical activation of the prepared powder was studied using high-energy planetary milling. The microstructure and dielectric properties of the sintered ceramics in both the milled and unmilled forms were investigated.

2. Experimental procedures

$BaTiO_3$ has been prepared from stoichiometric proportions of barium acetate (99.6% purity, Fisher ChemAlert® Guide, USA) and titanium dioxide (98% purity, BDH Chemicals Ltd. Poole, England) precursors. $Ba(CH_3COO)_2$ was completely dissolved in distilled water and then the TiO_2 powder was added and mixed using a magnetic stirrer hot plate. The mixture was then dried in the oven (NEY Furnace, M-525) at 90°C for 24h. The dried powder was divided into two parts. One part was mixed with ethyl alcohol and milled in a planetary mill (Retsch PM400-Fritsch, Germany) for 7.5h and then designated as *milled* powder. The second part was left dried and designated as *unmilled* powder. Both powders were then calcined in air (Carbolite Furnace, GPC 1300, UK) at 950°C/2h. The prepared powders were die-pressed and sintered in air at different temperatures. The densities of the sintered ceramics were measured by the Archimedes' method. The microstructure and grain size of the as-sintered samples were investigated using a scanning electron microscope (SEM: JEOL, JSM 5400, Japan). X-ray diffractometer

(XRD-3A, Shimadzu-Japan, CuKα-Ni filter) was used for phase analysis. The sintered samples were coated on both faces with silver paste. The dielectric properties of the sintered ceramics were studied at different temperatures and frequencies using RCL meter (Philips, PM6304).

3. Results and discussions

3.1 Density and microstructure

The samples made from the calcined milled $Ba(CH_3COO)_2$-TiO_2 powder mixture were noted as S_M, and those made from the calcined unmilled one were named S_U. The SEM micrographs of S_M and S_U specimens sintered at 1300°C/3h are shown in Figure 1(a, b), respectively. Figure 1 (a) shows significant densification and grain growth for the S_M specimen. The sintered density of S_M was 5.108 g/cm3 (85% of the TD) and the average grain size was about 5μm. On the other hand, S_U specimen shows very fine grains and porous structure. The sintered density of S_U was 4.41 g/cm^3 (73.3% of the TD). These low values of the sintered densities, even for S_M specimen, may be due to the agglomeration of the starting powder. Consequently, the resulting microstructure contained large pores which could not be eliminated during conventional sintering. Consequently, this caused some difficulties in obtaining dense ceramics. The compact made from the unmilled powder that was sintered at 1350°C and designated as S_{UH} showed a relatively higher sintered density of 5.41 g/cm^3 (89.85% of the TD). The specimen exhibited a fine-grained structure with an average grain size of about 2μm and a fine porosity (Figure 2). This microstructure is quite similar to that obtained for compacts made from a nanocrystalline powder (Kim *et al*., 2004).

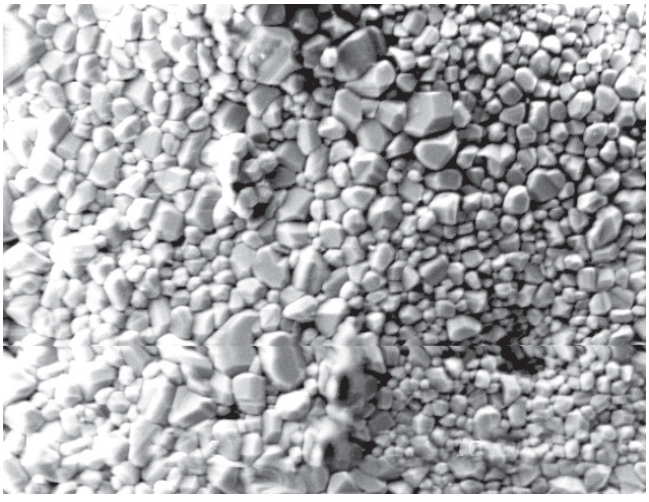

(a) S_M

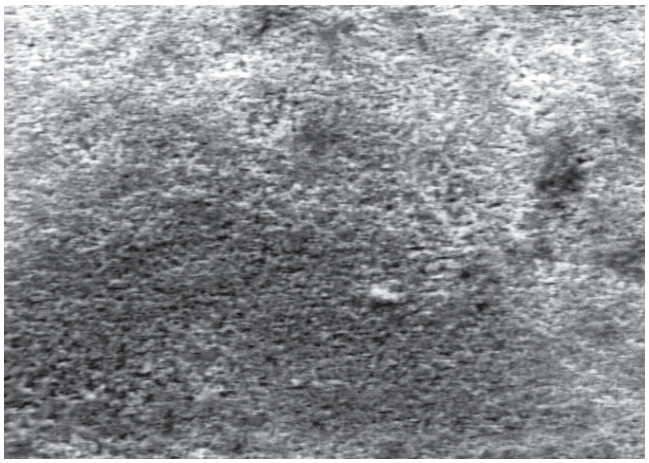

(b) S_U

Fig. 1. SEM micrographs S_M and S_U, compacts sintered at 1300°C/3h

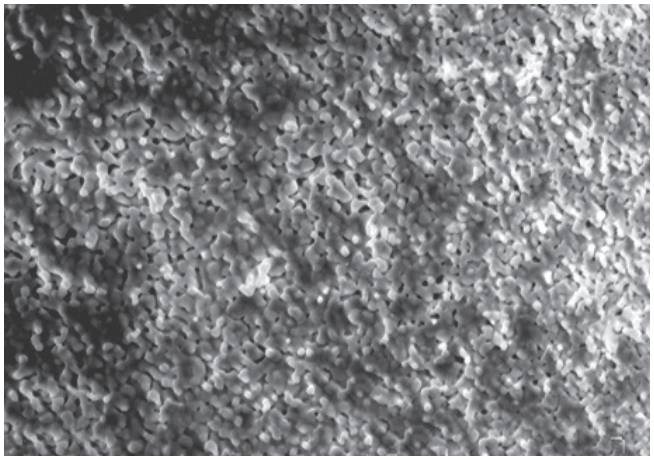

(a) X 1000

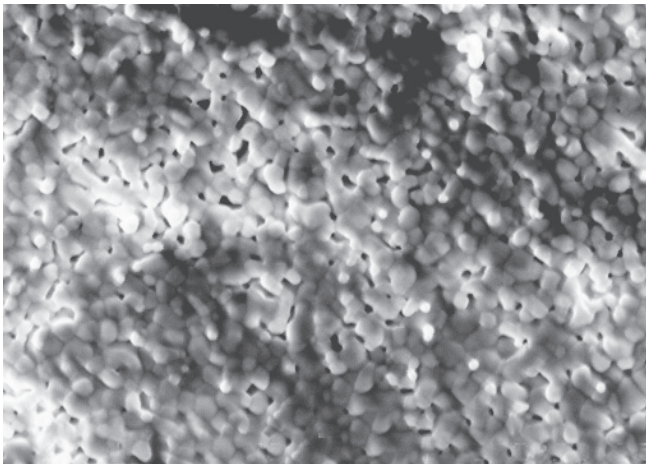

(b) X1700

Fig. 2. SEM micrographs of $BaTiO_3$ compact made from the unmilled powder and sintered at 1350°C/2h (S_{UH})

3.2 X-ray diffraction

Figures 3 & 4 show the x-ray diffraction patterns of the sintered compacts made from the milled and unmilled powders, respectively. Figure 3 shows that for the S_M specimen, a single phase of $BaTiO_3$ was formed after sintering at 1300°C/3h. On the other hand, for the compact made from the unmilled powder (S_U) and sintered at the same temperature, an extra peak occurs at 28.6° 2^thita which corresponds to a secondary phase of Ba_2TiO_4 (Figure 4). This phase is located most probably at the grain boundaries of the sintered compacts. The homogenization via diffusion process during sintering in the unmilled specimen is slower relative to the milled one. Milling improves homogeneity and accelerates the formation of $BaTiO_3$ at a relatively lower temperature, consequently preventing the secondary phase formation. Othman *et al*. 2014 reported that, if the complete formation of $BaTiO_3$ does not occur below 900°C (during the powder calcination), the formation of the secondary phase becomes favored. This secondary phase, as well as porosities, might inhibit grain growth and result in a barrier layer of intergranular microstructure. These results are in agreement with those obtained by Mukherjee *et al*. (2002).

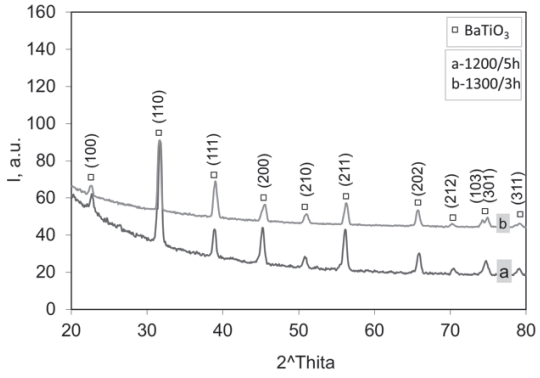

Fig. 3. XRD patterns of S_M specimens sintered at different temperatures

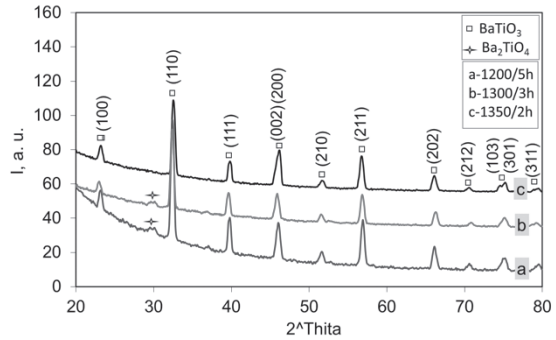

Fig. 4. XRD patterns for compacts made from the unmilled powder sintered at different temperatures

3.3 Dielectric properties

Figures 5, 6 and 7 show the variations of relative permittivities and dissipation factors with temperatures for S_M, S_U and S_{UH} specimens, respectively, and which are measured at different frequencies. Figure 5 shows that the S_M specimen has a relative permittivity of 2430 with a high dissipation factor of 0.5 at room temperature. It was measured at 500Hz. At Curie temperature (122°C), a well-defined permittivity peak was observed for this specimen. It had a higher relative permittivity of 8720 and low dissipation factor of 0.07, at the same frequency. Relative permittivity and the dissipation factor decrease upon increasing frequency at room temperature, while at Curie temperature, the frequency has no measurable effect on either. In contrast, a completely different behavior is noticed for the permittivity/temperature measurements obtained from the unmilled powder samples. The S_U specimen sintered at 1300°C showed lower relative permittivity values at all temperatures (Figure 6). These lower values were attributed to its higher porosity and poor densification. However, upon increasing the sintering temperature to 1350°C/3h, the S_{UH} sample gave higher relative permittivity values at room temperature (5626, measured at 500 Hz) and it showed broadening in the permittivity peaks at 50°C and 122°C (Figure 7). This might be due to the effect of core/shell morphology of the unmilled powder that results from a thin layer of a secondary phase at the grain boundaries. Deshpande *et al*. 2006 reported that the presence of Ba-rich phase increases the stress in the material, consequently enhancing the room temperature dielectric constant, and causing broadening in the permittivity peaks at the Curie temperature. Xu & Gao (2004) obtained similar results for $BaTiO_3$ ceramic made from hydrothermally prepared powder. They attributed this outcome to the content of the tetragonal phase. However, it should be noted that they were using excess barium in their starting precursors (Ba/Ti was 1.6), which might be a source of a thin Ba-rich grain boundary layer. This factor could account for the increase of the aforementioned dielectric constants.

The broadening in the permittivity peaks at 50°C and 122°C for S_{UH} is typical for the diffuse transition of the orthorhombic to tetragonal phase at the lower temperature and of the tetragonal phase to the cubic phase at the Curie temperature. Previous research shows that the high temperature peak corresponds to the $BaTiO_3$ core, while the low temperature peak corresponds to the grain boundary phase as a shell (Lin *et al*., 2007).

A Debye-like relaxation behavior could be explained by the Maxwell-Wagner relaxation at the interfaces between grains and their boundaries. Raevski *et al*. (2003) used a simple relaxation model of Maxwell-Wagner to describe a two-component material having different dielectric permittivities: ε_1 and ε_2. They concluded that the overall permittivity (ε) is controlled by the permittivity (ε_2) of the thin layer of thickness t at the grain boundary of a grain of size d according to the following equation:

$$\varepsilon = \frac{d\varepsilon_2}{t}$$

The remarkable increase in the permittivity values of the S_{UH} specimen relative to the S_M specimen might be explained using Raevski's equation given above, taking into consideration the decrease of the grain boundary phase with the sintering temperature (Figure 4). While, in the case of S_M, the milling of the powder is thought to destroy the shell layer formed during preparation, leading to the dielectric behavior that was mentioned. This is a similar result to that obtained for the classically prepared $BaTiO_3$ by solid state reaction between barium carbonate and titanium dioxide (Lokare, 2015).

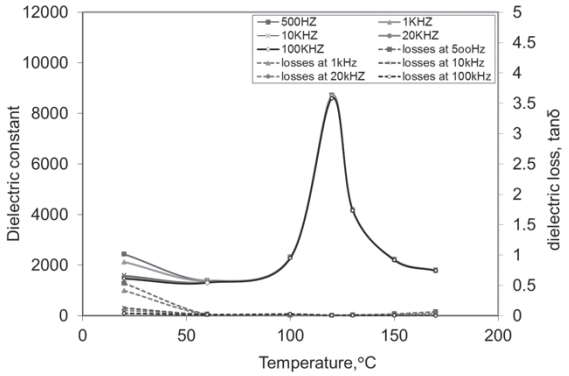

Fig. 5. Dielectric properties of S_M compact, sintered at 1300°C/3h

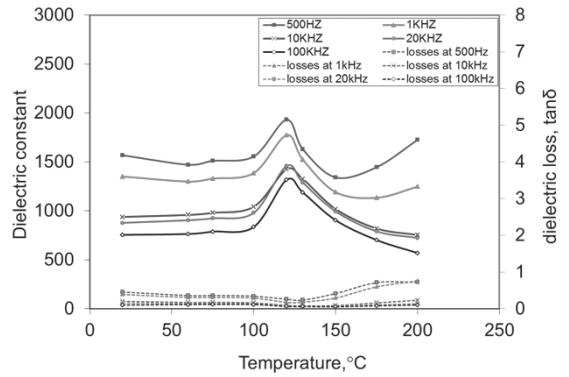

Fig. 6. Dielectric properties of S_U compact, sintered at 1300°C/3h

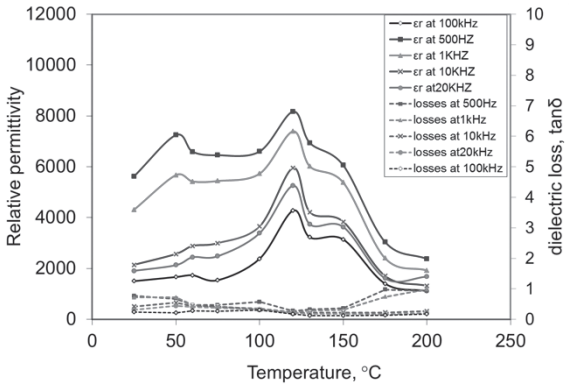

Fig. 7. Dielectric properties of S_{UH} compact, sintered at 1350°C/2h

3.4 Curie-Weiss behavior

The dielectric behavior can be characterized by Curie-Weiss law (Kittel, 1967):

$$\varepsilon = \varepsilon_o + \frac{C}{T - T_c}$$

Where: C is the Curie constant, T_c is the Curie temperature, ε_o is the permittivity of the free space (8.85 x10^{-14} Farads/cm).

Figures 8, 9 and 10 show the changes in the reciprocal of permittivity with a temperature above the Curie temperature for the samples S_M, S_U, and S_{UH}, respectively. The S_M sample showed a first-order phase transition at Curie temperature and typical Curie-Weiss behavior, as deduced from the linear relationship of the reciprocal of the permittivity vs. temperature above T_c (Figure 8). From the slope of this line, the Curie constant could be calculated. It was found to be 1.25x10^5 (at 1kHz), a figure in agreement with the values reported for this material (Marković *et al*., 2009). The calculated Curie constants for S_U and S_{UH} specimens were nearly similar to that of the S_M specimen at low frequencies. However, their Curie constants decreased with frequencies. A decrease in linearity as expressed by the R^2 values (Figs. 9 and 10), where R is the correlation coefficient, may lead to a conclusion that these samples do not strictly follow the Curie-Weiss law. In order to calculate the degree of the dielectric dispersion and diffuseness, a modified Curie-Weiss equation was proposed by Uchino & Nomura (1982).

$$\frac{1}{\varepsilon_r} - \frac{1}{\varepsilon_m} = \frac{(T - T_m)^{\gamma}}{C'},$$

where ε_r is the relative permittivity and ε_m is the maximum relative permittivity, T_m, γ and C' are constants. The parameter γ gives information on the character of phase

transition, where γ =1 for normal Curie-Weiss behavior, and γ =2 for the complete diffuse transition. γ can be determined from the slope of the straight line plot of ln (1/ ε_r -1/ ε_m) vs. ln (T-T_m). Figure 11(a, b) shows an example of this plot for the dielectric measurements for the S_{UH} specimen at 500 Hz and 100 kHz, respectively. The γ-values obtained from the figure, were 1.3 and 1.29, respectively.

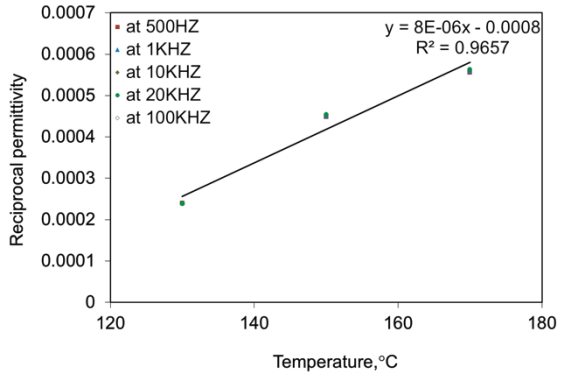

Fig. 8. Reciprocal of relative permittivity versus temperature at T > Tc for S_M

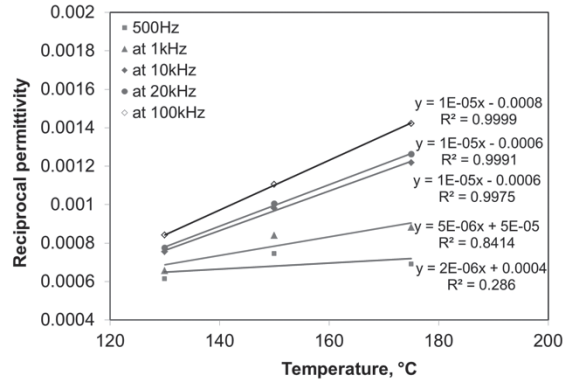

Fig. 9. Reciprocal of relative permittivity versus temperature at T > T_c for S_U

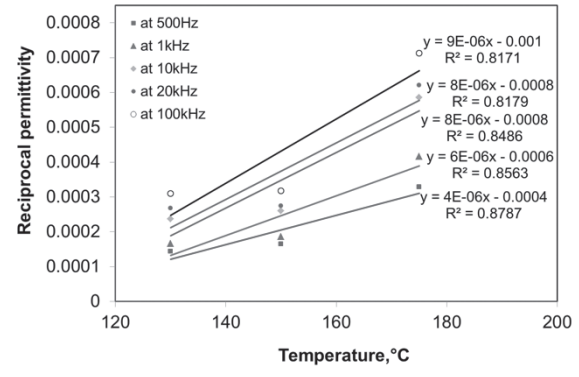

Fig. 10. Reciprocal of relative permittivity versus temperature at T > T_c for S_{UH}

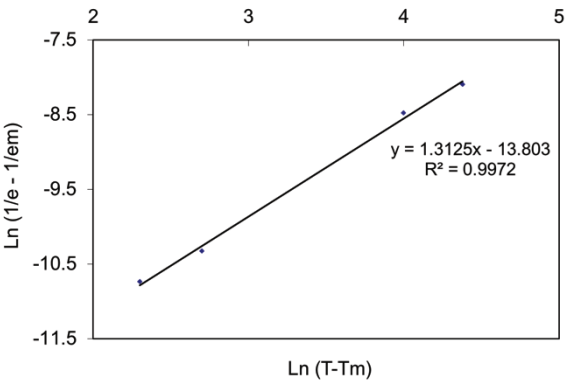

(a)

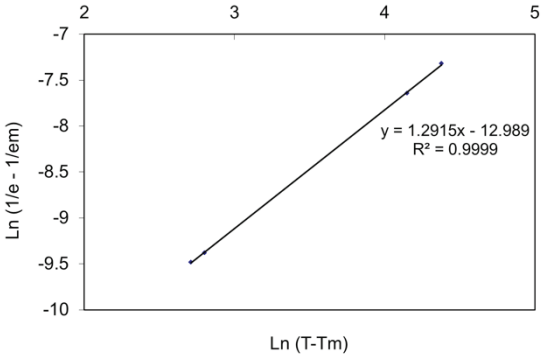

(b)

Fig. 11. Plot of the logarithm of reciprocal of relative permittivities versus ln (T-T_m) for S_{UH} at: (a) 500 Hz and (b) 100kHz

4. Conclusions

Densification and dielectric properties of barium titanate prepared from titanium dioxide and barium acetate aqueous solutions in both the unmilled and milled forms have been studied. From this research, the following conclusions can be made:

1. The compacts made from the milled powder sintered to a higher density compared to the unmilled powder.
2. The sample made from the milled powder showed a permittivity of 2430 at room temperature and a maximum of 8720 at Curie temperature.
3. The permittivities of the compact made from the unmilled powder sintered at 1350°C/2h were 5626 and 8170 at RT and Curie temperature, respectively.
4. A core shell morphology of the S_{UH} sample having a thin Ba-rich phase at the grain boundaries, accounts for the high permittivities at room temperature.

5. The sintered compacts made from the unmilled powder showed dielectric relaxor-like behavior and had relatively stable permittivity over a wide range of temperatures.

6. Milling of powder gives a better homogeneity, but it destroys the shell layer and results in a classic barium titanate dielectric behavior.

7. The results obtained in this work for the unmilled powder could be useful in the manufacture of barrier layer capacitors.

References

Deshpande, S.R., Potdar, H.S., Patil, M. M., Deshpande, V. V. & Khollam, Y.B. (2006). Dielectric properties of $BaTiO_3$ ceramics prepared from powders with bimodal distribution. Journal of Industrial Engineering and Chemistry, **12**(4): 584-588.

Ertuğ, B. (2013). The overview of the electrical properties of barium titanate. American Journal of Engineering Research, **02**(08): 01-07.

Gomes, M., Magalhães, L.G., Paschoal, A.R., Macedo, Z.S. & Lima, Á.S., *et al.* (2018). An eco-friendly method of $BaTiO_3$ nanoparticle synthesis using coconut water. Journal of Nanomaterials, **2018**: 1-7.

Kim, H.T. & Han, Y.H. (2004). Sintering of nanocrystalline BaTiO3. Ceramics International, **30**: 1719-172.

Kittel, C. (1967). Introduction to solid state physics. 3rd Ed. Chapter 15, pp. 456. John Wiley, Hoboken, NJ.

Kong, L.B., Ma, J., Huang, H., Zhang, R. F. & Que, W.X. (2002). Barium titanate derived from mechanochemically activated powders. Journal of Alloys and Compounds, **337**: 226-230.

Li, B., Wang, X. & Li, L.U. (2002). Synthesis and sintering behavior of $BaTiO_3$ prepared by different chemical methods. Materials Chemistry and Physics, **78**: 292–298.

Lin, L., Fan, H., Fang, F. & Jim, L. (2007). Electrical heterogeneity in $CaCu_3Ti_4O_{12}$ ceramics fabricated by sol-gel method. Solid State Communications, **142** (10): 573-576.

Lokare, S.A. (2015). Structural and electrical properties of $BaTiO_3$ prepared by Solid State Route. International Journal of Chemical and Physical Sciences, ISSN: 2319-6602 IJCPS, Special Issue ETP, **4**: 154-161.

Luan, W., Gao, L., Kawaoka, H., Sekino, T. & Niihara, K. (2004). Fabrication and characteristics of fine-grained $BaTiO_3$ ceramics by spark plasma sintering. Ceramics International, **30**: 405–410.

Marković, S., Miljković, M., Jovalekić, C., Mentus, S. & Uskoković. D. (2009). Densification, microstructure and electrical properties of $BaTiO_3$ (BT) ceramics prepared from ultrasonically de-agglomerated BT powders. Materials and Manufacturing Processes, **24** (10-11): 1114-1123.

Mukherjee, N. Roseman, R.D. & Zhang, Q. (2002). Sintering behavior and PTCR properties of stoichiometric blend $BaTiO_3$. Journal of Physics and Chemistry of Solids, **63**: 631-638.

Othman, K.I., Hassan, A.A., Abdelal, O.A.A., Elshazly, E.S. & Ali M. E-S., *et al.* (2014). Formation mechanism of barium titanate by solid-state reactions. International Journal of Scientific & Engineering Research, **5** (7): 1460-1465.

Peng, Z. & Chen, Y. (2003). Preparation of $BaTiO_3$ nanoparticles in aqueous solutions. Microelectronic Engineering, **66**:102-106.

Raevski, I.P., Prosandeev, S.A., Bogatin, A. S. & Malitskaya, M.A. (2003). High dielectric permittivity in $AFe_{1/2}B_{1/2}O_3$ nonferroelectric perovskite ceramics (A=Ba, Sr, Ca $_{and}$ B=Nb,Ta,Sb). Journal of Applied Physics, **93**(7): 4130-4136.

Rotaru, R., Peptu, C., Samoila, P. & Harabagiu, V. (2017). Preparation of ferroelectric barium titanate through an energy effective solid state ultrasound assisted method. Journal of the American Ceramic Society, **100**: 4511 - 4518.

Uchino, K. & Nomura, S. (1982). Critical exponents of the dielectric constants in diffused-phase transition crystals. Ferroelectric Letters, **(44)**: 55-61.

Vijatović, M.M., Bobić, J.D. & Stojanović, B.D. (2008). History and Challenges of Barium Titanate: Part I. Science of Sintering. **40**: 155-165.

Xu, H. & Gao, L. (2004) Hydrothermal synthesis of high-purity $BaTiO_3$ powders: Control of powder phase and size, sintering density and dielectric properties. Materials Letters, **58**: 1582 - 1586.

Zheng, S. (2016). First-principles calculations of Ca/F co-doped anatase TiO_2. Kuwait Journal of Science, **43**(2): 162-171.

Submitted: 20/11/2018
Revised: 26/12/2018
Accepted: 06/01/2019

خصائص العزل الكهربي لتيتانات الباريوم المُحضرة من خليط من أسيتات الباريوم وثانى أكسيد التيتانيوم

[1،*]كلثوم اسماعيل عثمان، [1]مصطفى محمود السيد، [1]سامية إمام الحوت
قسم الفلزات، مركز البحوث النووية، هيئة الطاقة الذرية
المؤلف: *Kolthoum.O@yahoo.com*

الملخص

فى هذا البحث تمت دراسة عملية التلبيد والبناء الدقيق وخواص العزل الكهربى لتيتانات الباريوم المُحضرة من خليط من اسيتات الباريوم المائية وثانى أكسيد التيتانيوم المطحونة وغير المطحونة. وقد استخدمت تقنيات الميكروسكوب الالكترونى وحيود الأشعة السينية فى دراسة البناء الدقيق وحجم الحبيبات والأطوار البللورية. وقد وُجد اختلاف كبيرفى البناء الدقيق وخصائص العزل الكهربى بين العينات الملبدة من المساحيق المطحونة وغير المطحونة. وأظهرت العينات المُعدة من تيتانات الباريوم غير المطحونة ذروة عريضة عند درجة حرارة كورى وقيم مرتفعة للنفاذية الكهربية (5630) عند درجة حرارة الغرفة. وقد أُعزى ذلك إلى وجود طبقة رقيقة غنية بالباريوم تعمل كغلاف على حبيبات تيتانات الباريوم. كما أن العينات أظهرت سلوك عزل استرخائى مع نفاذية كهربية ثابتة نسبياً على نطاق واسع من درجات الحرارة. وعلى الرغم من أن عملية طحن المسحوق أعطت تجانساً جيداً إلا أنها أدت إلى تحطيم طبقة الغلاف وأدت إلى سلوك فى الخصائص الكهربية مشابه لتيتانات الباريوم التقليدية.